Electronic Supplementary Material (ESI) for Organic & Biomolecular Chemistry.
This journal is © The Royal Society of Chemistry 2014

Electronic Supplementary Information (ESI)

Ferrocene-pyrylium dyad as a selective colorimetric chemodosimeter for the toxic cyanide and hydrogen sulfide anions in water

---

Antonia Sola, Alberto Tárraga* and Pedro Molina*

Departamento de Química Orgánica; Universidad de Murcia; Campus de Espinardo; 30100 Murcia, Spain. Fax: +34 868 884 149; Tel: +34 868 887 496 and +34 868 887 499; E-mail: pmolina@um.es; E-mail: atarraga@um.es

Table of contents

Experimental section S3

Experimental procedures S4

^{1}H- and ^{13}C-NMR of 4-ferrocenyl-2,6-dimethylpyrylium **1** S5

^{1}H- and ^{13}C-NMR of (2*E*,4*E*)-4-ferrocenyl-2-methyl-6-oxohepta-2,4-dienenitrile **2** S6

^{1}H- and ^{13}C-NMR of 4-ferrocenyl-2,6-dimethylthiopyrylium **3** S7

Figure ESI 1 CV and OSWV of **1** in CH_3CN S8

Figure ESI 2. CV and OSWV of 4-ferrocenyl-2,6-dimethylthiopyrylium hexafluorophosphate in CH_3CN. S8

Figure ESI 3. Evolution of the CV of **1** in presence of 1 equiv. of CN^- in CH_3CN. S9

Figure ESI 4. OSWV for **1**, **1**+CN^- and 4-ferrocenyl-2,6-dimethyl thiopyrylium hexafluorophosphate in CH_3CN. S9

Figure ESI 5. Changes in the spectrum of **1** upon addition of increasing amounts of CN^-, HS^- and OH^- and subsequent addition of HBF4 in CH_3CN. S10

Figure ESI 6. Changes in the absorption spectrum of **1** upon addition of increasing amounts of CN^- in CH_3CN. S10

Figure ESI 7. Changes in the absorption spectrum of **1** upon addition of increasing amounts of HS^- in H_2O and CH_3CN. S11

Figure ESI 8. Changes in the absorption spectrum of **1** upon addition of increasing amounts of OH^- in H_2O and CH_3CN. S11

Figure ESI 9. Semilogarithmic plot for determining the detection limit of **1** towards CN^- and HS^-. S12

Figure ESI 10. ESI-MS spectrum of the species obtained upon addition of KCN to **1**. S12

Figure ESI 11. ESI-MS spectrum of 4-ferrocenyl-2,6-dimethyl thiopyrylium hexafluorophosphate. S13

Table 1.- Electrochemical data of the species formed upon addition of amines S13

Figure ESI 12. Evolution of CV and OSWV in the presence of **1** alkyl amines. S14

Figure ESI 13. Evolution of the absorption spectrum of **1** upon addition of increasing amounts of alkyl amines S14

Experimental Section.-

General Comments.- Melting point was measured on a hot-plate melting point apparatus and are uncorrected. ^{1}H- and ^{13}C-NMR spectra were recorded at 300 and 75 MHz, respectively. Chemical shifts refer to signals of tetramethylsilane in the case of ^{1}H and ^{13}C spectra. The following abbreviations were used to represent the multiplicity of the signals: s (singlet), d (doublet), m (multiplet), st (pseudotriplet), q (quaternary carbon atom).

UV-vis spectra were carried out in a UV-vis-NIR spectrophotometer using a dissolution cell of 10 mm path. The samples were solved in CH_3CN or in H_2O ($c = 1x10^{-4}$ M) and the spectra were recorded with the spectra background corrected before and after of the sequential additions of aliquots of 0.25 equiv of anions in H_2O ($c = 2.5x\ 10^{-2}$ M).

CV and OSWV techniques were performed with a conventional three-electrode configuration consisting of platinum working and auxiliary electrodes and a Ag/AgCl reference electrode. The experiments were carried out with a solution of **1** in CH_3CN ($c = 5x10^{-4}$ M) containing 0.1 M $(n\text{-}C_4H_9)_4PF_6$ ($TBAPF_6$) as supporting electrolyte. All the potential values reported are relative to the decamethylferrocene (DCMF) couple at room temperature. Deoxygenation of the solutions was achieved by bubbling nitrogen for at least 10 min and the working electrode was cleaned after each run. The cyclic voltammograms were recorded with a scan rate increasing from 0.05 to 1.00 Vs^{-1}, while the OSWV were recorded at a scan rate of 100 mVs^{-1} with a pulse high of 10 mV and a step time of 50 ms. Typically, a solution of the receptor ($c = 5\ x\ 10^{-4}$ M in CH_3CN) containing $TBAPF_6$ as supporting electrolyte (0.190 g) was used. The guest under investigation was then added as a H_2O solution ($c = 2.5x10^{-2}$ M) using a microsyringe whilst the cyclic voltammetric properties of the solution were monitored. DCMF was used as an external reference both for potential calibration and for reversibility criteria.

Experimental procedures.-

Preparation of 4-ferrocenyl-2,6-dimethylthiopyrylium hexafluorophosphate 3.-. To a solution of 4-ferrocenyl-2,6-dimethylpyrylium hexafluorophosphate (0.050 g, 0.11 mmol) in CH_3CN (50 ml) a solution of NaSH (0.013 g, 0.22 mmol) in H_2O (5 ml) was added. The reaction mixture was stirred at room temperature for 15 min and then HBF_4. (0.01 g, 0.11 mmol) was added dropwise. After stirring at room temperature for 15 min the solvent was removed under reduced pressure and the resulting crude product was triturated with dry ethyl ether (25 ml), giving rise to a green solid which was crystallized from acetonitrile-diethyl ether (1:10). Mp 238-240 ºC (d). (Found: C, 44.70; H, 3.48. Calc. for $C_{17}H_{17}F_6FePS$: C, 44.96; H, 3.77%). δ_H (300 MHz, CD_3CN, Me_4Si) 8.03 (2H, s, thiopyrylium ring), 5.28 (2H, st, Fc), 5.21 (2H, st, Fc), 4.26 (5H, s, Fc), 2.73 (6H, s, Me). δ_C (75 MHz, CD_3CN, Me_4Si) 24.6 (CH_3), 72.2 (2xCH, Fc), 74.2 (5xCH, Fc), 79.4 (2xCH, Fc), 80.3 (q, Fc), 131.2 (CH), 165.7 (q), 168.6 (q). ESI-MS: *m/z* 309 (M^+, 100%).

Preparation of (2*E*,4*E*)-4-ferrocenyl-2-methyl-6-oxohepta-2,4-dienenitrile 2.-. To a solution of 4-ferrocenyl-2,6-dimethylpyrylium hexafluorophosphate (0.050 g, 0.11 mmol) in CH_3CN (50 ml) a solution of Bu_4NCN (0.022 g, 0.22 mmol) in H_2O (5 ml) was added. The reaction mixture was stirred at room temperature for 15 min and then the solvent was removed under reduced pressure and the resulting crude product was triturated with dry ethyl ether (25 ml), giving rise to a pink solid which was crystallized from acetonitrile-diethyl ether (1:10). Mp 255-258 ºC (d). (Found: C, 67.50; H, 5.09; N, 4.72. Calc. for $C_{18}H_{17}FeNO$: C, 67.73; H, 5.37; N, 4.39 %). δ_H (400 MHz, CD_3CN, Me_4Si) 7.22 (1H, m), 6.67 (1H, d, *J* =1.5 Hz), 4.61 (2H, st, Fc), 4.47 (2H, st, Fc), 4.21 (5H, s, Fc), 2.18 (3H, s, Me), 2.11 (3H, d, *J* = 1.5 Hz, Me). δ_C (100 MHz, CD_3CN, Me_4Si) 20.6 (CH_3), 31.0 (CH_3), 68.9 (2xCH, Fc), 70.9 (5xCH, Fc), 72.0 (2xCH, Fc), 112.1 (q, Fc), 119.0 (q), 122.9 (CH), 144.4 (CH), 150.0 (q), 197.6 (q). ESI-MS: *m/z* 320.0781 (M^++1, 57%)

4-Ferrocenyl-2,6-dimethylpyrylium hexafluorophosphate 1

^{1}H NMR (400 MHz, CD_3CN, Me_4Si)

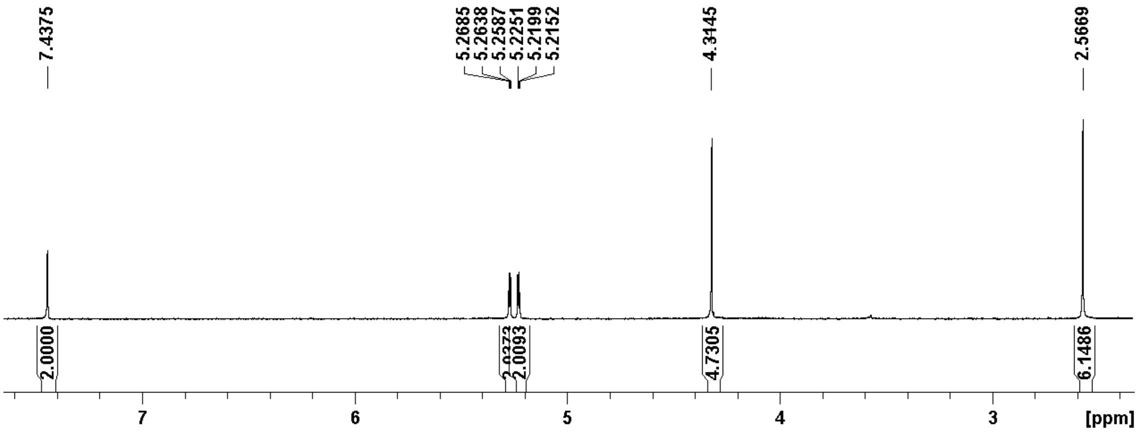

^{13}C NMR (100 MHz, CD_3CN, Me_4Si) (see also ref. 20 within the main text)

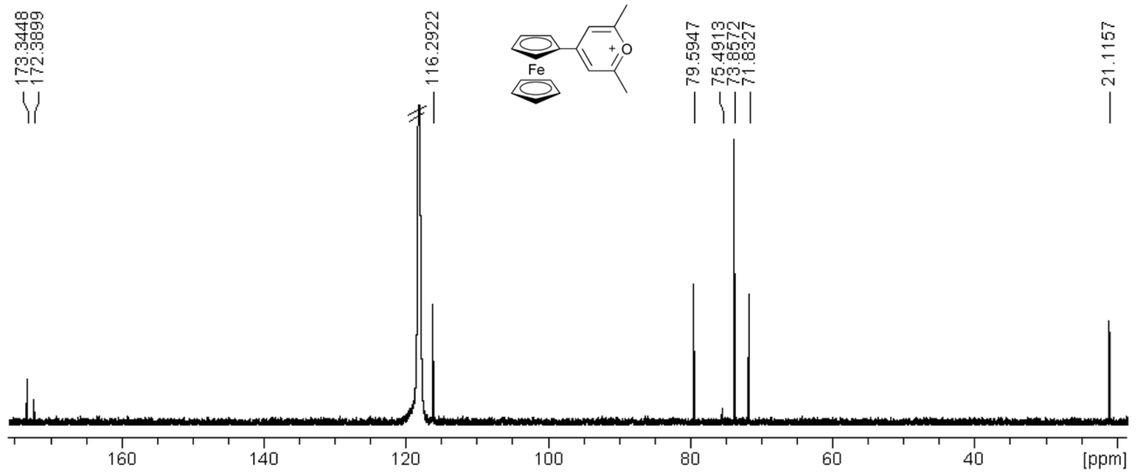

(2*E*,4*E*)-4-Ferrocenyl-2-methyl-6-oxohepta-2,4-dienenitrile 2

^{1}H NMR (400 MHz, CD_3CN, Me_4Si)

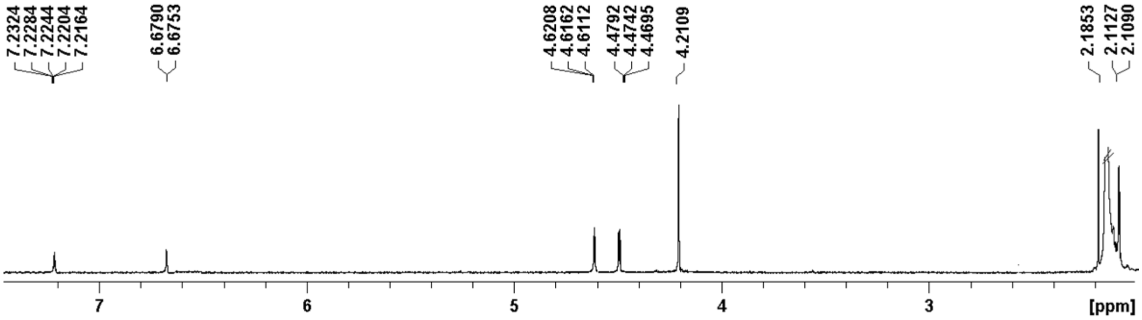

^{13}C NMR (100 MHz, CD_3CN, Me_4Si)

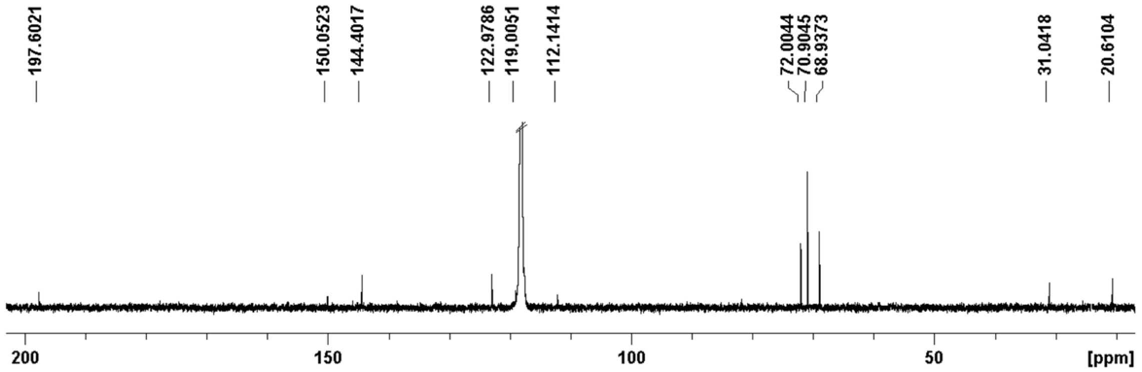

4-Ferrocenyl-2,6-dimethylthiopyrylium hexafluorophosphate 3.-

^{1}H NMR (300 MHz, CD$_3$CN, Me$_4$Si)

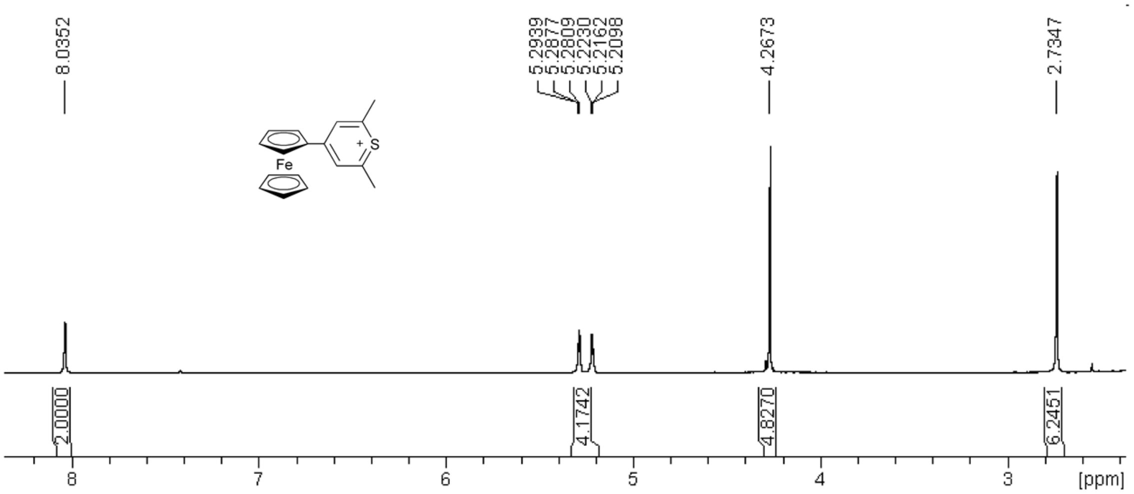

^{13}C NMR (75 MHz, CD$_3$CN, Me$_4$Si)

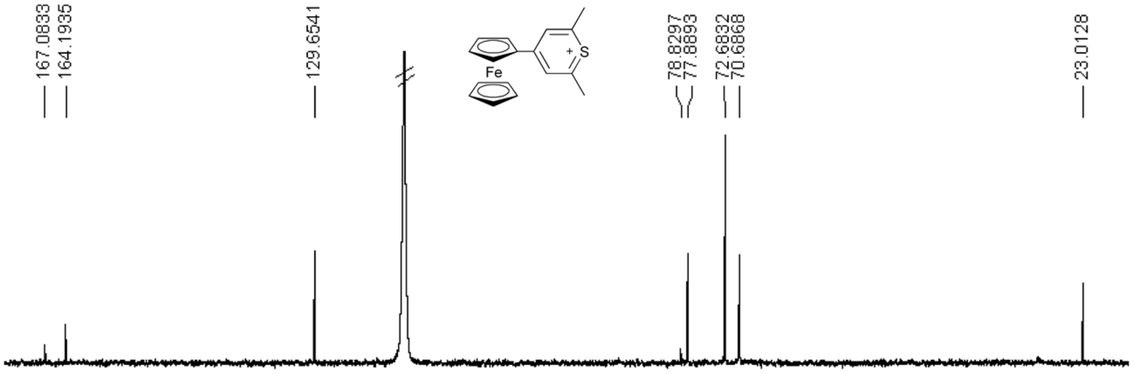

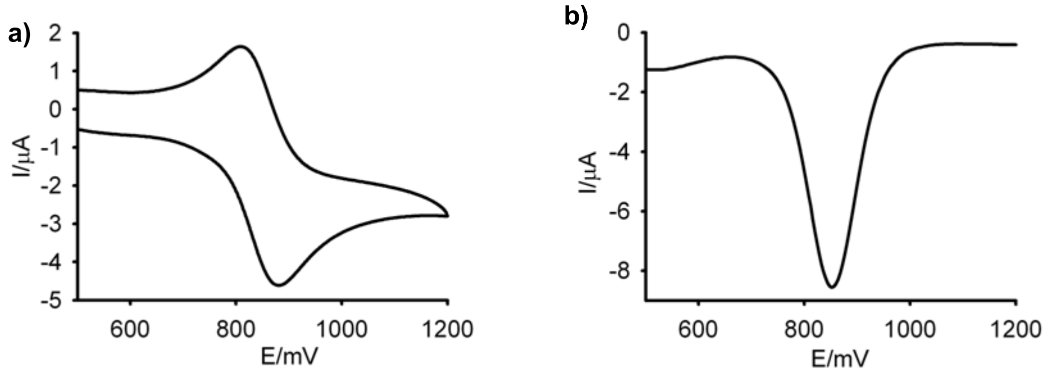

Figure ESI 1. CV (a) and OSWV (b) of **1** (c = 5·10^{-4}M in CH_3CN) using $[(n\text{-}Bu)_4N]PF_6$ as supporting electrolyte.

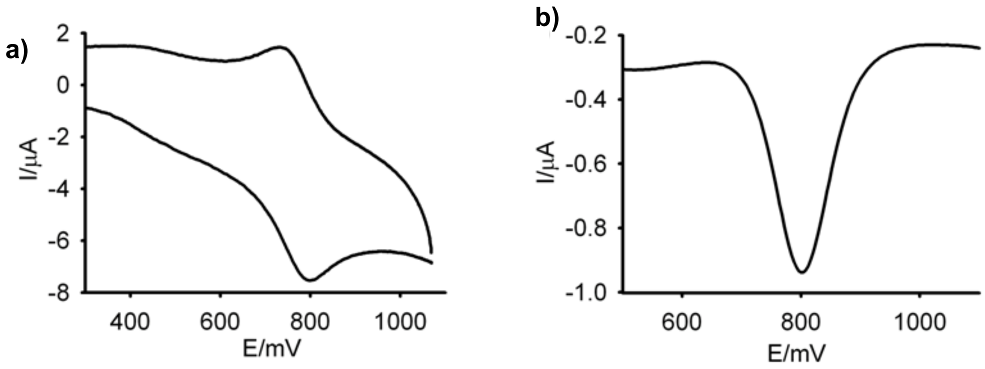

Figure ESI 2. CV (a) and OSWV (b) of 4-ferrocenyl-2,6-dimethylthiopyrylium hexafluorophosphate (c = 5·10^{-4}M in CH_3CN) using $[(n\text{-}Bu)_4N]PF_6$ as supporting electrolyte.

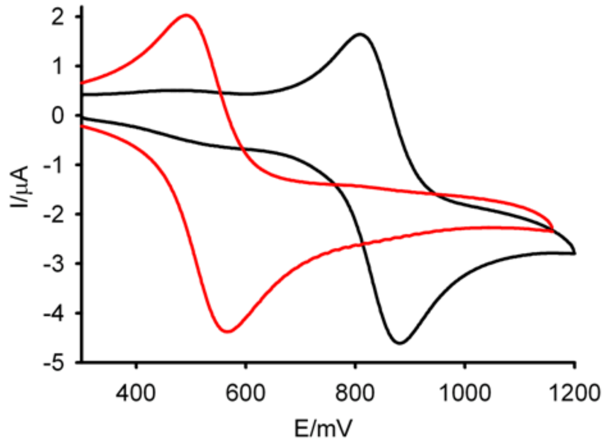

Figure ESI 3. CV of **1** (c = $5 \cdot 10^{-4}$M in CH_3CN) (black) scanned at 0.1 $V \cdot S^{-1}$ in the presence of 1 equiv. of $[(n\text{-Bu})_4N]CN$ (c = $2.5 \cdot 10^{-2}$M in H_2O) (red) using $[(n\text{-Bu})_4N]PF_6$ as supporting electrolyte.

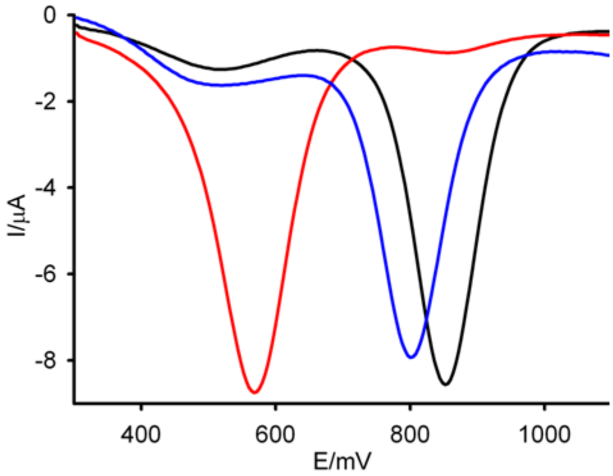

Figure ESI 4. OSWV of **1** (black), **1** upon addition of 1 equiv of $[(n\text{-Bu})_4N]CN$ (red) and 4-ferrocenyl-2,6-dimethylthiopyrylium hexafluorophosphate (blue) (c = $5 \cdot 10^{-4}$M in CH_3CN) using $[(n\text{-Bu})_4N]PF_6$ as supporting electrolyte.

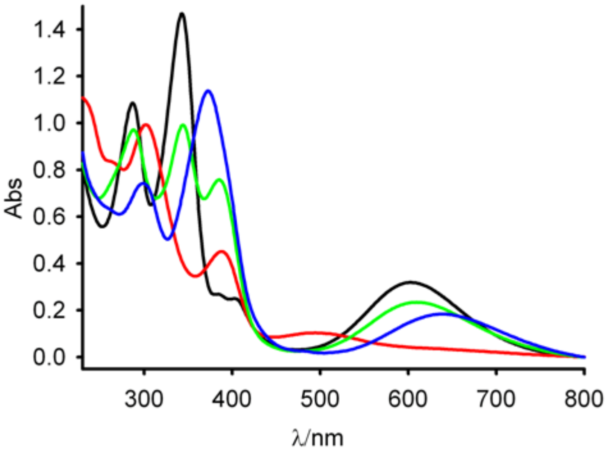

Figure ESI 5. Evolution of the absorption spectrum of **1** (c = 1x10^{-4} M in CH_3CN) (black) upon addition of increasing amounts of CN^- (red), HS^- (blue) and OH^- (green), in water, and subsequent addition of HBF_4.

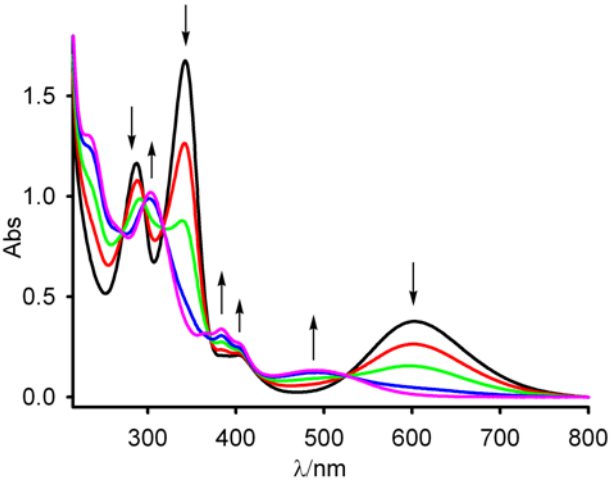

Figure ESI 6. Evolution of the absorption spectra of **1** (black) (c =1·10^{-4} M in CH_3CN) upon addition of increasing amounts of CN^- anion, until 1 equiv. was added (pink). Arrows indicate absorptions that increase or decrease during the experiment.

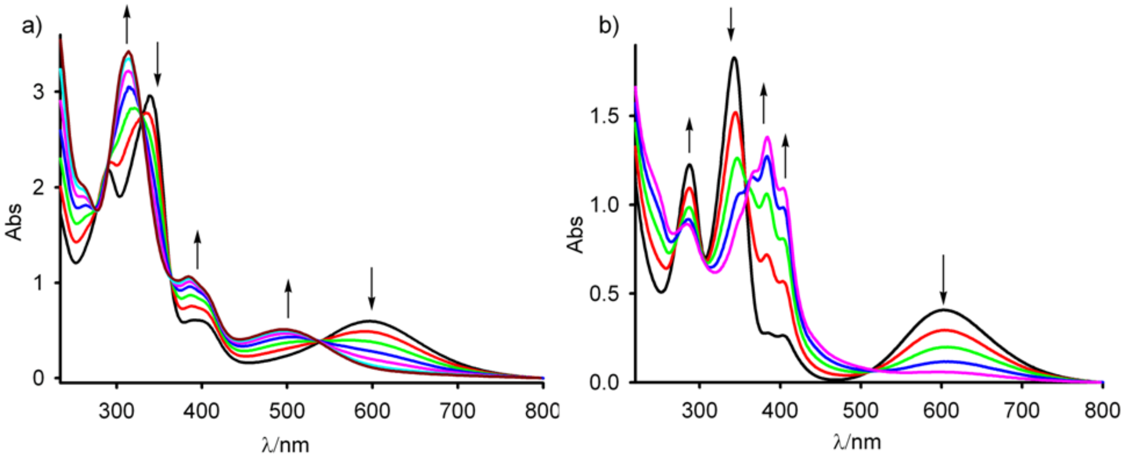

Figure ESI 7. Evolution of the absorption spectra of **1** (black) (c =1·10^{-4} M) in a) H_2O and b) CH_3CN upon addition of increasing amounts of HS^- anion, until 1 equiv was added. Arrows indicate absorptions that increase or decrease during the experiment.

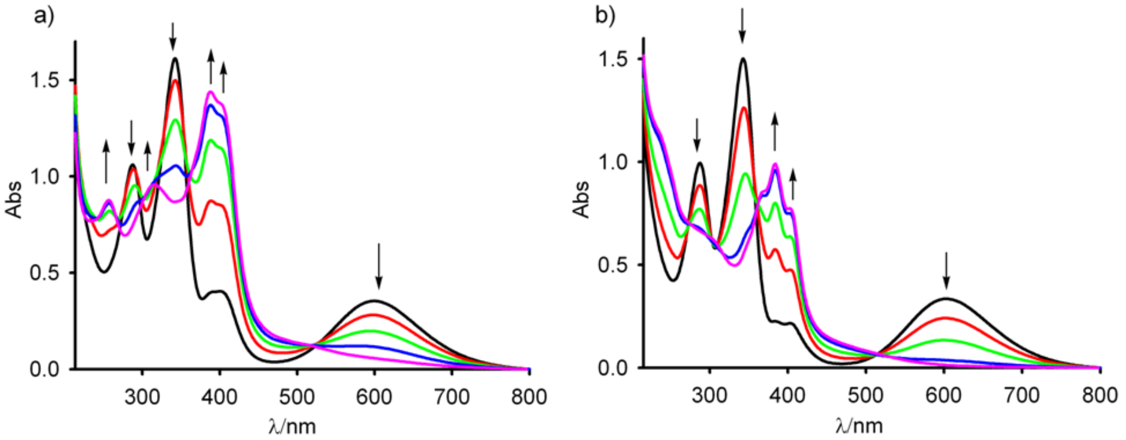

Figure ESI 8. Evolution of the absorption spectra of **1** (black) (c =1·10^{-4} M) in a) H_2O and b) CH_3CN upon addition of increasing amounts of OH^- anion, until 1 equiv. was added. Arrows indicate absorptions that increase or decrease during the experiment.

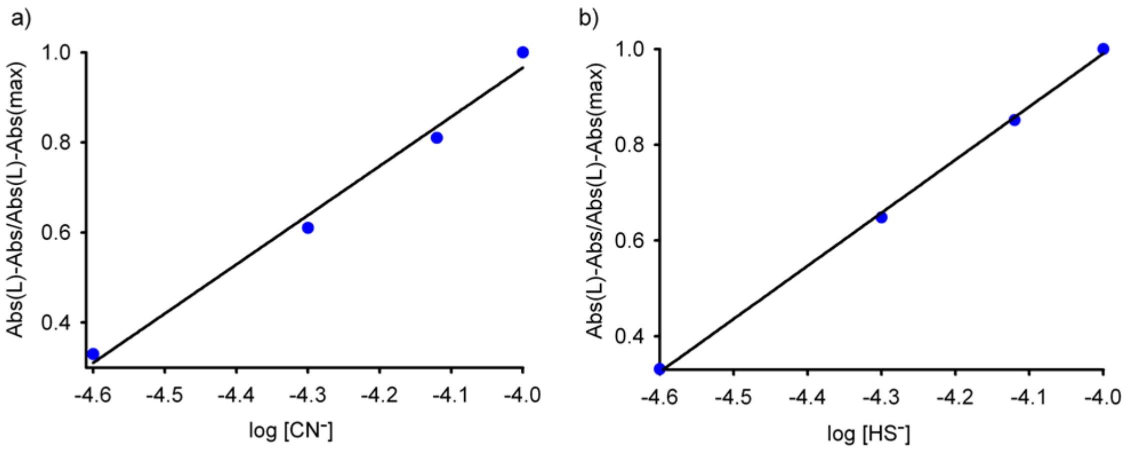

Figure ESI 9. Absorbance of **1** ($c = 1\cdot10^{-4}$M in H_2O) at each concentration of a) CN^- y b) HS^- added, normalized between the minimum absorbance, found at zero equiv of anion, and the maximum absorbance.

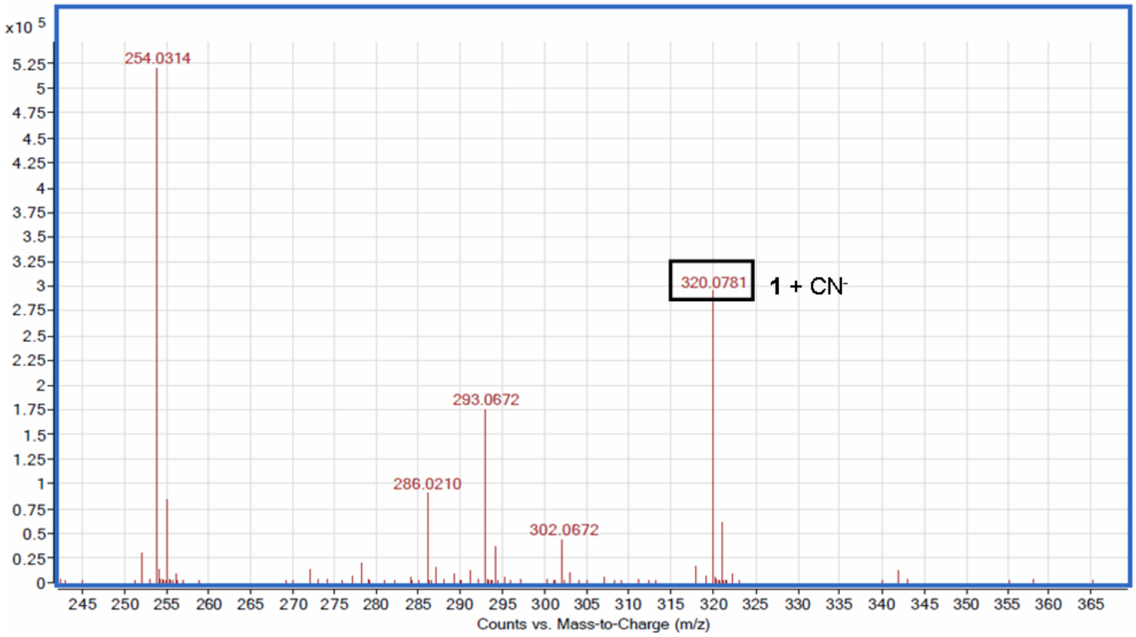

Figure ESI 10. ESI-MS spectrum of the species obtained upon addition of 1 equiv of KCN to a CH_3CN solution of **1**

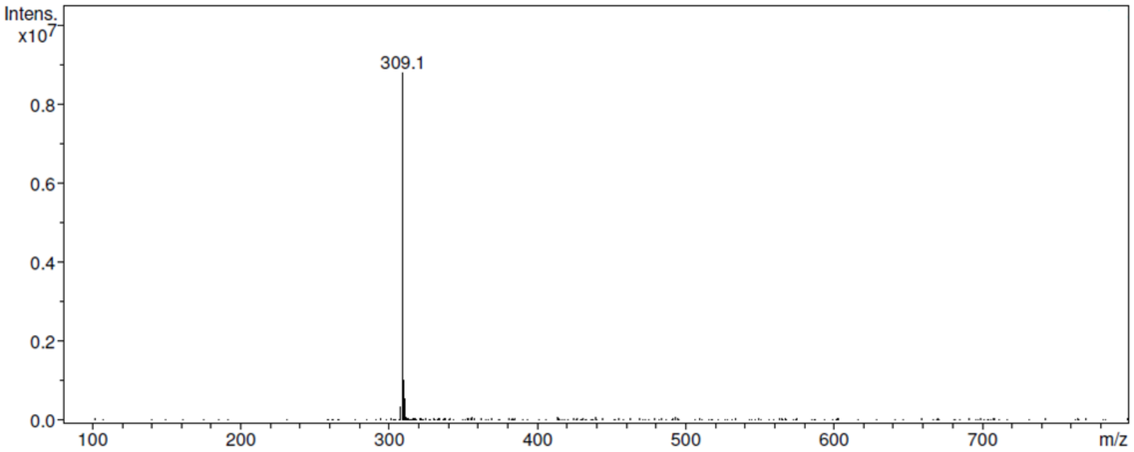

Figure ESI 11. ESI-MS spectrum of 4-ferrocenyl-2,6-dimethylthiopyrylium hexafluorophosphate

Table 1. Electrochemical data of the free receptor **1** and the species formed upon addition of different amines

	$E_{1/2}$ (mV)	$\Delta E_{1/2}$ (mV)
1	850	---
1 + pentylamine	690	-160
1 + hexylamine	690	-160
1 + cyclohexylamine	690	-160
1 + benzylamine	690	-160
1 + 2-methyl-4-nitroaniline	850	0
1 + 2-methyl-4-nitroaniline	850	0
1 + 4-chloro-2-methylaniline	850	0
1 + 2-aminobenzimidazole	850	0

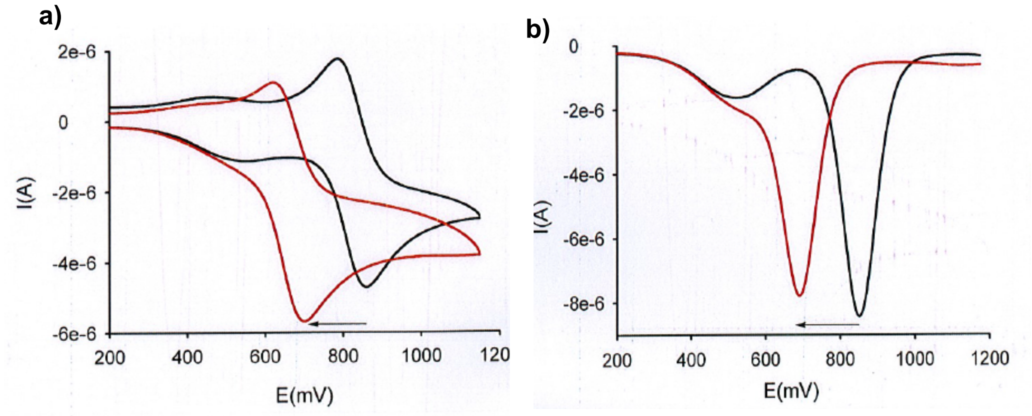

Figure ESI 12. Evolution of CV (a) and OSWV (b) of **1** (c = $5 \cdot 10^{-4}$M in CH_3CN) (black) using $[(n\text{-}Bu)_4N]PF_6$ as supporting electrolyte upon addition of alkyl amines (red).

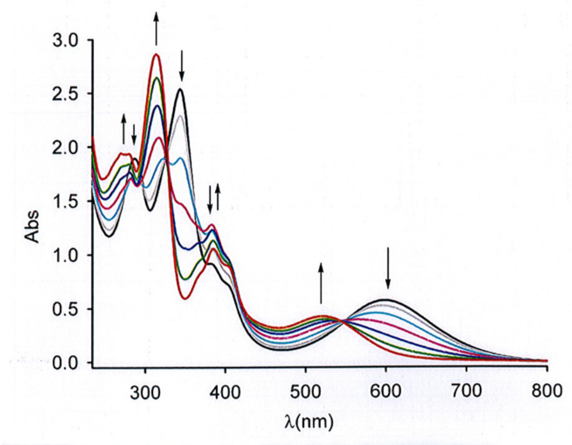

Figure ESI 13. Evolution of the absorption spectrum of **1** (c = 1×10^{-4} M in CH_3CN) (black) upon addition of increasing amounts of alkyl amines.